

Impact of genetic alterations on central nervous system progression of primary vitreoretinal lymphoma

Kota Yoshifuji,^{1*} Daichi Sadato,^{2*} Takashi Toya,³ Yotaro Motomura,¹ Chizuko Hirama,² Hiroshi Takase,⁴ Kouhei Yamamoto,⁵ Yuka Harada,⁶ Takehiko Mori¹ and Toshikage Nagao¹

¹Department of Hematology, Graduate School of Medical and Dental Sciences, Tokyo Medical and Dental University (TMDU); ²Clinical Research Support Center, Tokyo Metropolitan Komagome Hospital; ³Hematology Division, Tokyo Metropolitan Komagome Hospital;

⁴Department of Ophthalmology and Visual Science, Graduate School of Medical and Dental Sciences, Tokyo Medical and Dental University (TMDU); ⁵Department of Pathology, Graduate School of Medical and Dental Sciences, Tokyo Medical and Dental University and ⁶Clinical Laboratory, Tokyo Metropolitan Komagome Hospital, Tokyo, Japan

**KYo and DS contributed equally as first authors.*

Correspondence: K. Yoshifuji
yoshhema@tmd.ac.jp

Received: January 1, 2024.

Accepted: May 24, 2024.

Early view: June 6, 2024.

<https://doi.org/10.3324/haematol.2023.284953>

©2024 Ferrata Storti Foundation

Published under a CC BY-NC license



Supplementary data

Supplemental Method

Treatment for the patients

All patients underwent initial treatment with weekly intravitreal MTX injections (400 $\mu\text{g}/100 \mu\text{L}$) in the affected eyes until the lesions resolved. Thereafter, systemic HD-MTX (3.5 g/m² every other week for a total of five cycles) was administered to 20/36 patients, and the remainder were carefully observed without any additional chemotherapy, according to the decision of the physician. If the treatment was not tolerated, it was discontinued at the discretion of the physician.

Flow cytometry analysis

The infiltrating cells were isolated from the vitreous humor and obtained for flow cytometry. The surface expression of B-cell markers (CD19 and CD20), T-cell markers (CD3, CD4, CD5, and CD8), and κ and λ light chains were examined. Using the criteria suggested by Levy et al.¹, we defined a monoclonal κ population as one where the κ/λ ratio was 3:1 or greater, and monoclonal λ population as one that had a λ/κ ratio in excess of 2:1.

PCR analysis of IGH rearrangement

PCR analysis of IGH rearrangement was outsourced to LSI Medience Corporation (Tokyo, Japan).

Cytokine measurement

The IL-6 and IL-10 concentrations in a vitreous humor were measured at our laboratory and SRL Corporation (Tokyo, Japan). In total, 50 μL of vitreous supernatant from each patient was used for ELISA according to the given manufacturer instructions (Invitrogen, Camarillo, CA, USA).

Amplicon-based targeted sequencing

The custom gene panel of 107 genes frequently mutated in lymphoma, and PVRL was designed using Illumina Design Studio. Covered bases were 406,093 bp, and there were 3,044 (5–157 amplicons/gene)

designed panel amplicons. This custom gene panel was designed to cover all exons of each gene on genomic DNA. As a template, 10 ng DNA amplified the target genes. Libraries were synthesized using AmpliSeq Library Plus for Illumina (Illumina, San Diego, CA, USA). The libraries were analyzed using MiSeq Reagent Kit v2 (500 cycles) with MiSeq (Illumina) platform following the provided manufacturer instructions.

Whole exome sequencing

Genomic DNA capture, enrichment, and elution were performed using Agilent SureSelect Human V6 (Agilent Technologies, Santa Clara, CA) following protocols by the manufacturer. In total, 600 ng of each genomic DNA sample was used as bait. After ligation on adaptor oligonucleotides, tail repairing, and purification, libraries were quantified by qPCR to obtain an adequate DNA template for sequencing. Synthesized libraries were sequenced on the NovaSeq 6000 (Illumina) as 150 bp pair-ended reads. Sequencing was performed by Rhexia (Tokyo, Japan).

Gene variant discovery

Fastq files from next-generation sequencing were cleaned with Trimmomatic,² and the results were aligned to the human reference genome, hg19, using Burrows–Wheeler Alignment (BWA)³. Qualimap⁴ was used to analyze coverages of mapped reads. Gene variants were detected using HaplotypeCaller included in the GATK tool⁵. Gene variants obtained from HaplotypeCaller were filtered with the parameters of quality/depth, mapping quality, and strand bias to exclude false-positive variants.⁶ Variants were annotated with information from the Refseq, 1000G, and Exac databases in Illumina VariantStudio 3.0 software (Illumina). Variants with a prevalence of >1% in each regional population were excluded. COSMIC and CLINVAR databases and previous genomics research papers (Table S1) were referred to judge whether the variants were pathogenic or not.

Detection of copy number alteration

Copy number alteration for each PVRL sample were analyzed using CNVkit⁷ with bam files generated by the mapping process of gene variant discovery. Consequently, the normalized coverage values of PVRL data were compared to that of uveitis cases as controls and gene copy numbers were obtained. During the

calculation process, the number of amplicons and the \log_2 value in control data (-5 or less) and spread of read depth (1 or more) were applied as a filter, resulting in copy number of read depth (20 or more) with low spread read depth gene regions. The \log_2 copy number of >0.25 was decided as gain and the \log_2 copy number less than -0.25 was considered as loss. CNA of *HIST1H1B*, *HIST1H1C*, *HIST1H1E*, *HIST1H4H*, and *SOCS1* were excluded from the analysis because the copy number variation between the samples was too large. In the annotation process, copy number gain of oncogene and loss of tumor suppressor gene were defined as pathogenic and incorporated into analysis. Genes with the gain of function mutations had oncogenic function were considered as oncogenes, and genes with the loss of function mutations contributed to tumorigenic pathway were considered as tumor suppressor genes (Table S1).

Table S1. Target genes included in the sequencing panel of 107 genes and the reference used for gene annotation

Gene	Mutation effect	Characteristics of mutations	Reference
<i>ACTB</i>	N.I.	Missense in N-terminal	Lohr et al ⁸ , Wang et al ⁹
<i>APC</i>	Loss of function	-	Zhang et al ¹⁰ , Schmitz et al ¹¹
<i>ARID1A</i>	Loss of function	-	Zhang et al ¹⁰ , Schmitz et al ¹¹
<i>ARID2</i>	Loss of function	-	Wang et al ⁹
<i>AXIN1</i>	N.I.	-	Wang et al ⁹
<i>ATM</i>	Loss of function	-	Schmitz et al ¹¹
<i>B2M</i>	Loss of function	-	Challa-Malladi et al ¹² , Schmitz et al ¹¹
<i>BCL10</i>	N.I.	-	Morin et al ¹³ , Schmitz et al ¹¹
<i>BCL2</i>	Gain of function	-	Morin et al ¹³ , Wang et al ⁹
<i>BCL6</i>	N.I.	-	Morin et al ¹³ , Schmitz et al ¹¹
<i>BCL7A</i>	Loss of function	Missense in N-terminal	Schmitz et al ¹¹ , Baliñas-Gavira et al ¹⁴
<i>BRCAl</i>	Loss of function	-	Wang et al ⁹
<i>BRAF</i>	Gain of function	Missense in hotspot (e.g. V600)	Schmitz et al ¹¹
<i>BTG1</i>	Loss of function	Missense in N-terminal	Lee et al ¹⁵ , Bonzheim et al ¹⁶ , Mlynarczyk et al ¹⁷
<i>BTG2</i>	Loss of function	Missense in N-terminal	Lee et al ¹⁵ , Bonzheim et al ¹⁶ , Wang et al ⁹ , Mlynarczyk et al ¹⁷
<i>CACNA1C</i>	N.I.	-	Lee et al ¹⁵
<i>BTK</i>	Loss of function	-	Lohr et al ⁸ , Schmitz et al ¹¹ , Hu et al ¹⁸
<i>CCND3</i>	Loss of function	Missense in C-terminal hotspot	Morin et al ¹³ , Schmitz et al ¹⁹ , Schmitz et al ¹¹
<i>CD274</i>	Gain of function	-	Kataoka et al ²⁰ , Schmitz et al ¹¹
<i>CD58</i>	Loss of function	-	Challa-Malladi et al ¹² , Schmitz et al ¹¹
<i>CD70</i>	Loss of function	-	Schmitz et al ¹¹
<i>CD79A</i>	Gain of function	Missense in immunoreceptor tyrosine-based activation motif	Davis et al ²¹ , Schmitz et al ¹¹
<i>CD79B</i>	Gain of function	Missense in immunoreceptor tyrosine-based activation motif (e.g. Y196)	Davis et al ²¹ , Bonzheim et al ¹⁶ , Wang et al ⁹
<i>CDKN2A</i>	Loss of function	-	Nayyar et al ²² , Wang et al ⁹
<i>CDKN2B</i>	Loss of function	-	Nayyar et al ²² , Wang et al ²¹
<i>CIITA</i>	Loss of function	-	Mottok et al ²³ , Wang et al ⁹
<i>CREBBP</i>	Loss of function	-	Bonzheim et al ¹⁶ , Wang et al ⁹
<i>CSMD1</i>	Loss of function	-	Escudero-Esparza et al ²⁴ , Lee et al ¹⁵
<i>CXCR4</i>	Gain of function	Nonsense in C-terminal hotspot (e.g. S342*)	Treon et al ²⁵ , Lee et al ¹⁵
<i>DTX1</i>	Loss of function	-	de Miranda et al ²⁶ , Lee et al ¹⁵
<i>DUSP2</i>	N.I.	-	Lee et al ¹⁵ , Wang et al ⁹
<i>EHD1</i>	N.I.	-	Lee et al ¹⁵
<i>EP300</i>	Loss of function	-	Schmitz et al ¹¹
<i>ERBB4</i>	Gain of function	-	Wang et al ⁹
<i>ETS1</i>	Loss of function	-	Morin et al ¹³ , Bonetti et al ²⁷ , Wang et al ⁹
<i>ETV6</i>	Loss of function	-	Bonzheim et al ¹⁶ , Wang et al ⁹
<i>EZH2</i>	Gain of function	-	Zhang et al ¹⁰ , Schmitz et al ¹¹
<i>FAS</i>	Loss of function	-	Grønbaek et al ²⁸ , Schmitz et al ¹¹
<i>FAT1</i>	Loss of function	-	Laginestra et al ²⁹ , Wang et al ⁹
<i>FAT4</i>	Loss of function	-	Cai et al ³⁰ , Lee et al ¹⁵
<i>FBXW7</i>	Loss of function	-	Wang et al ⁹

<i>FLT3</i>	Gain of function	Missense in thymidine kinase domain (e.g. D835)	Wang et al ⁹
<i>FLT4</i>	Gain of function	Missense in thymidine kinase domain	Liu et al ³¹ , Wang et al ⁹
<i>FOXO1</i>	Loss of function	Missense in phosphoinositide 3-kinase/AKT phosphorylation sites	Trinh et al ³² , Wang et al ⁹
<i>FRY</i>	Loss of function	-	Lee et al ¹⁵ , Mai et al ³³
<i>GADD45B</i>	N.I.	-	Wang et al ⁹
<i>GNA13</i>	Loss of function	-	Muppidi et al ³⁴ , Schmitz et al ¹¹
<i>GRHR</i>	Loss of function	-	Lee et al ¹⁵ , Andrades et al ³⁵
<i>HIST1H1B</i>	Loss of function	-	Li et al ³⁶ , Lee et al ¹⁵
<i>HIST1H1C</i>	Loss of function	-	Li et al ³⁶ , Lee et al ¹⁵
<i>HIST1H1E</i>	Loss of function	-	Li et al ³⁶ , Lee et al ¹⁵
<i>HIST1H4H</i>	Loss of function	-	Li et al ³⁶ , Lee et al ¹⁵
<i>IGLL5</i>	Loss of function	-	Bonzheim et al ¹⁶ , Lee et al ¹⁵
<i>IKZF3</i>	Loss of function	-	Wang et al ⁹
<i>IRF4</i>	Loss of function	Missense in DNA binding domain	Cherian et al ³⁷ , Lee et al ¹⁵ , Bonzheim et al ¹⁶ , Wang et al ⁹
<i>IRF8</i>	Loss of function	Missense in DNA binding domain	Reddy et al ³⁸ , Lee et al ¹⁵
<i>ITPKB</i>	Loss of function	-	Schmitz et al ¹¹
<i>KLHL14</i>	Loss of function	-	Choi et al ³⁹ , Lee et al ¹⁵
<i>KLHL6</i>	Loss of function	-	Schmitz et al ¹¹
<i>KMT2D</i>	Loss of function	-	Lee et al ¹⁵ , Wang et al ⁹
<i>LRP1B</i>	Loss of function	-	Lee et al ¹⁵
<i>LRIG1</i>	N.I.	-	Lee et al ¹⁵
<i>MCL1</i>	N.I.	-	Wang et al ⁹
<i>MED12</i>	N.I.	-	Wang et al ³⁸
<i>MEF2B</i>	N.I.	-	Pon et al ⁴⁰ , Wang et al ⁹
<i>MALT1</i>	N.I.	-	Schmitz et al ¹¹
<i>MPEG1</i>	Loss of function	-	Schmitz et al ¹¹ , Lee et al ¹⁵
<i>MUC16</i>	N.I.	-	Lee et al ¹⁵
<i>MTOR</i>	Loss of function	-	Schmitz et al ¹¹
<i>MYC</i>	Gain of function	-	Wang et al ⁹
<i>MYD88</i>	Gain of function	-	Lee et al ¹⁵ , Bonzheim et al ¹⁶ , Wang et al ⁹
<i>NFKB1</i>	Loss of function	-	Wang et al ⁹
<i>NF1</i>	Loss of function	-	Schmitz et al ¹¹
<i>NFKBIA</i>	Loss of function	-	Schmitz et al ¹¹ , Weniger et al ⁴¹
<i>NFKBIE</i>	Loss of function	-	Schmitz et al ¹¹ , Weniger et al ⁴¹
<i>NFKBIZ</i>	N.I.	-	Schmitz et al ¹¹
<i>NOTCH1</i>	Gain of function	-	Schmitz et al ¹¹
<i>NOTCH2</i>	Gain of function	-	Schmitz et al ¹¹
<i>OSBPL10</i>	N.I.	-	Dobashi et al ⁴² , Lee et al ¹⁵
<i>OTOF</i>	N.I.	-	Lee et al ¹⁵
<i>PCDH15</i>	N.I.	-	Lee et al ¹⁵
<i>PAX5</i>	Loss of function	-	Schmitz et al ¹¹ , Gu et al ⁴³
<i>PIM1</i>	Loss of function	-	Lee et al ¹⁵ , Bonzheim et al ¹⁶ , Wang et al ⁹
<i>PLCG2</i>	N.I.	-	Wang et al ⁹
<i>PRDM1</i>	Loss of function	-	Bonzheim et al ¹⁶ , Wang et al ⁹
<i>RBMX</i>	Loss of function	-	Schmitz et al ¹¹ , Zheng et al ⁴⁴
<i>PTEN</i>	Loss of function	-	Schmitz et al ¹¹
<i>REL</i>	N.I.	-	Schmitz et al ¹¹
<i>RP1</i>	N.I.	-	Lee et al ¹⁵
<i>RUNX1</i>	Loss of function	-	Wang et al ⁹
<i>SETBP1</i>	Gain of function	-	Wang et al ⁹

<i>RHOA</i>	Gain of function	-	Schmitz et al ¹¹
<i>SGK1</i>	Gain of function	-	Schmitz et al ¹¹
<i>SOCS1</i>	Loss of function	-	Schmitz et al ¹¹
<i>SPEN</i>	Loss of function	-	Reddy et al ⁴⁰ , Schmitz et al ¹¹
<i>STAT3</i>	Gain of function	Missense in SH2 domain (e.g. Y640F, D661Y)	Koskela et al ⁴⁵ , Schmitz et al ¹¹
<i>STAT6</i>	Gain of function	Missense in DNA binding domain (e.g. D419)	Yildiz et al ⁴⁶ , Schmitz et al ¹¹
<i>TBL1XR1</i>	Loss of function	Missense in WD domain	Venturutti et al ⁴⁷ , Bonzheim et al ¹⁶ , Wang et al ⁹
<i>TCF3</i>	Gain of function	-	Schmitz et al ¹¹
<i>TET2</i>	Loss of function	-	Schmitz et al ¹¹
<i>TMSB4X</i>	N.I.	-	Lee et al ¹⁵
<i>TNFAIP3</i>	Loss of function	-	Kato et al ⁴⁸ , Schmitz et al ¹¹
<i>TNFRSF14</i>	Loss of function	-	Schmitz et al ¹¹ , Wu et al ⁴⁹
<i>TP53</i>	Loss of function	-	Schmitz et al ¹¹ , Wang et al ⁹
<i>UBALD2</i>	N.I.	-	Lee et al ¹⁵
<i>USH2A</i>	N.I.	-	Lee et al ¹⁵
<i>ZFP36L1</i>	Loss of function	-	Reddy et al ³⁸ , Lee et al ¹⁵

N.I., Not identified. Details of references were listed in supplementary references.

Table S2. Detected pathogenic genetic mutations

Case	Gene	Mutation type	cDNA change	AA change	VAF (%)	Read depth
1	<i>MYD88</i>	Missense	c.794T>C	p.Leu265Pro	29.36	453
1	<i>PIMI</i>	Frameshift	c.644_680delAGCCGGTGCAAGATCTCTTC GACTTCATCACGGAAAG	p.Glu215GlyfsTer138	20.99	567
1	<i>PIMI</i>	Nonsense	c.691C>T	p.Gln231Ter	40.71	565
1	<i>ETS1</i>	Nonsense	c.1323C>G	p.Tyr441Ter	27.11	439
1	<i>CD79B</i>	Missense	c.590A>G	p.Tyr197Cys	27.89	882
1	<i>BTG2</i>	Missense	c.133G>T	p.Ala45Ser	14.31	1,139
10	<i>TBL1XR1</i>	Missense	c.1108G>T	p.Asp370Tyr	55.50	582
10	<i>PIMI</i>	Splice	c.513+1G>C		57.03	619
10	<i>PRDM1</i>	Splice	c.291G>C	p.Glu97Asp	58.21	1,029
10	<i>PRDM1</i>	Splice	c.291+1G>A		58.41	1,029
10	<i>CDKN2A</i>	Missense	c.247C>T	p.His83Tyr	64.08	710
10	<i>ETV6</i>	Splice	c.33+1G>A		71.48	519
10	<i>CD79B</i>	Missense	c.590A>G	p.Tyr197Cys	78.99	2,385
10	<i>KLHL14</i>	Nonsense	c.289C>T	p.Gln97Ter	44.37	978
10	<i>IGLL5</i>	Nonsense	c.64C>T	p.Gln22Ter	42.40	500
10	<i>BTG2</i>	Missense	c.142G>A	p.Glu48Lys	43.54	2,522
10	<i>BTG2</i>	Missense	c.157C>T	p.His53Tyr	35.65	3,669
10	<i>BTG1</i>	Missense	c.498G>A	p.Met166Ile	39.23	1,300
10	<i>BTG1</i>	Missense	c.398G>A	p.Ser133Asn	44.41	1,504
10	<i>BTG1</i>	Missense	c.208A>G	p.Ile70Val	40.31	2,079
10	<i>BTG1</i>	Missense	c.129C>A	p.Ser43Arg	46.29	283
12	<i>MYD88</i>	Missense	c.794T>C	p.Leu265Pro	28.17	1,260
12	<i>PIMI</i>	Frameshift	c.149_156delGCAACGCC	p.Arg50HisfsTer13	56.27	670
12	<i>PIMI</i>	Frameshift	c.276delG	p.Met92IlefsTer93	60.48	625
12	<i>PIMI</i>	Nonsense	c.676G>T	p.Glu226Ter	48.71	1,944
12	<i>PIMI</i>	Nonsense	c.720_748delGCAGGTGCTGGAGGCCCGTGC GGCACTGCC	p.Trp240Ter	24.73	1,326
12	<i>PRDM1</i>	Frameshift	c.500_522delCTCCCCGGGAGCAAAACCTG GCT	p.Ser167CysfsTer14	34.95	495
12	<i>ACTB</i>	Missense	c.143G>A	p.Gly48Asp	26.49	1,797
12	<i>ETV6</i>	Nonsense	c.19C>T	p.Gln7Ter	30.12	601
12	<i>ETV6</i>	Missense	c.1172A>G	p.Tyr391Cys	23.27	709
12	<i>BTG1</i>	Nonsense	c.103C>T	p.Arg35Ter	37.11	256

12	<i>KLHL14</i>	Frameshift	c.625_635delCTGGTGGAGGA	p.Leu209CysfsTer47	34.28	878
12	<i>KLHL14</i>	Nonsense	c.271C>T	p.Gln91Ter	29.34	634
12	<i>IGLL5</i>	Splice	c.206+2T>A		24.32	6,187
12	<i>BTG2</i>	Missense	c.83G>A	p.Gly28Asp	26.39	2,876
12	<i>BTG2</i>	Missense	c.185G>C	p.Gly62Ala	25.24	2,524
12	<i>BTG1</i>	Missense	c.304C>T	p.Leu102Phe	31.11	270
12	<i>BTG1</i>	Missense	c.116C>T	p.Thr39Ile	36.33	256
22	<i>MYD88</i>	Missense	c.794T>C	p.Leu265Pro	31.92	639
22	<i>TBLIXR1</i>	Missense	c.941T>A	p.Val314Asp	37.48	643
22	<i>HIST1H1B</i>	Missense	c.392C>G	p.Ala131Gly	73.16	395
22	<i>PIMI</i>	Nonsense	c.652C>T	p.Gln218Ter	48.17	546
22	<i>PRDM1</i>	Splice	c.291G>C	p.Glu97Asp	74.72	542
22	<i>CDKN2A</i>	Missense	c.197A>G	p.His66Arg	85.45	55
22	<i>PTEN</i>	Frameshift	c.149_153dupTTGAT	p.Asp52LeufsTer4	27.35	1,104
22	<i>MPEG1</i>	Nonsense	c.271C>T	p.Gln91Ter	33.27	505
22	<i>KMT2D</i>	Nonsense	c.6229C>T	p.Gln2077Ter	38.25	1,336
22	<i>CIITA</i>	Nonsense	c.657C>A	p.Cys219Ter	36.02	1,180
22	<i>CD79B</i>	Missense	c.590A>C	p.Tyr197Ser	34.73	976
26	<i>BTG2</i>	Nonsense	c.16G>T	p.Gly6Ter	47.99	2,761
26	<i>MYD88</i>	Missense	c.794T>C	p.Leu265Pro	39.86	1,041
26	<i>TBLIXR1</i>	Missense	c.1099T>C	p.Cys367Arg	38.34	866
26	<i>HIST1H1B</i>	Frameshift	c.230_257delAGAAGAATAACAGCCGCATT AAGCTGGG	p.Glu77AlafsTer6	18.61	1,752
26	<i>PIMI</i>	Nonsense	c.387C>G	p.Tyr129Ter	51.70	853
26	<i>PAX5</i>	Splice	c.41_46+13delGGACAGGTAGGACCGCGAT		35.36	1,151
26	<i>GRHPR</i>	Frameshift	c.129_130delGG	p.Glu44AlafsTer48	15.02	486
26	<i>GRHPR</i>	Frameshift	c.129_130delGG	p.Glu44AlafsTer48	15.02	486
26	<i>GRHPR</i>	Frameshift	c.129_130delGG	p.Glu44AlafsTer48	15.02	486
26	<i>MPEG1</i>	Nonsense	c.1201G>T	p.Glu401Ter	29.63	1,441
26	<i>MPEG1</i>	Frameshift	c.1195_1196delAA	p.Lys399ValfsTer10	36.38	1,443
26	<i>MPEG1</i>	Frameshift	c.920delG	p.Gly307AlafsTer21	29.60	1,108
26	<i>ETV6</i>	Splice	c.33+1G>C		57.42	404
26	<i>ETV6</i>	Nonsense	c.427C>T	p.Gln143Ter	54.02	1,405
26	<i>KMT2D</i>	Nonsense	c.14152G>T	p.Glu4718Ter	43.40	1,719
26	<i>CIITA</i>	Nonsense	c.1099C>T	p.Gln367Ter	30.15	617
26	<i>CIITA</i>	Frameshift	c.3052delG	p.Glu1018LysfsTer32	62.17	423

26	<i>BCL2</i>	Missense	c.351C>G	p.Ser117Arg	24.56	2,895
26	<i>BCL2</i>	Missense	c.20C>T	p.Thr71Ile	27.50	1,491
26	<i>GRHPR</i>	Frameshift	c.129_130delGG	p.Glu44AlafsTer48	15.02	486
26	<i>GRHPR</i>	Frameshift	c.129_130delGG	p.Glu44AlafsTer48	15.02	486
26	<i>BTG2</i>	Missense	c.96G>T	p.Glu32Asp	26.12	2,726
31	<i>MYD88</i>	Missense	c.794T>C	p.Leu265Pro	34.50	774
31	<i>TBLIXR1</i>	Missense	c.1051G>A	p.Glu351Lys	32.16	398
31	<i>TET2</i>	Frameshift	c.4745_4746delCT	p.Ser1582PhefsTer31	12.00	175
31	<i>PIMI</i>	Frameshift	c.201_214delGCACAGCCCCGGCT	p.His68ArgfsTer101	73.88	157
31	<i>PIMI</i>	Splice	c.513+1G>A		30.50	400
31	<i>PIMI</i>	Nonsense	c.652C>T	p.Gln218Ter	56.61	295
31	<i>PIMI</i>	Nonsense	c.691C>T	p.Gln231Ter	33.74	492
31	<i>PIMI</i>	Frameshift	c.711_724delCTTCTTCTGGCAGG	p.Phe238AlafsTer57	38.14	527
31	<i>PIMI</i>	Nonsense	c.1057G>T	p.Glu353Ter	24.67	608
31	<i>ETV6</i>	Splice	c.34-1G>A		29.54	799
31	<i>ETV6</i>	Splice	c.1254-2A>G		31.91	564
31	<i>KMT2D</i>	Nonsense	c.11911C>T	p.Gln3971Ter	33.17	612
31	<i>DTX1</i>	Nonsense	c.229C>T	p.Gln77Ter	32.22	239
31	<i>CD79B</i>	Missense	c.589T>C	p.Tyr197His	69.73	621
31	<i>BTG1</i>	Missense	c.347G>A	p.Gly116Glu	41.59	428
31	<i>BTG1</i>	Missense	c.145G>A	p.Ala49Thr	36.11	144
39	<i>MYD88</i>	Missense	c.794T>C	p.Leu265Pro	39.48	423
39	<i>KMT2D</i>	Nonsense	c.12844C>T	p.Arg4282Ter	34.29	35
49	<i>MYD88</i>	Missense	c.794T>C	p.Leu265Pro	46.60	515
49	<i>PIMI</i>	Nonsense	c.697G>T	p.Glu233Ter	73.22	956
49	<i>PIMI</i>	Frameshift	c.737_740delTGCG	p.Val246GlyfsTer118	73.17	954
49	<i>CD79B</i>	Missense	c.590A>C	p.Tyr197Ser	48.21	1,931
49	<i>KLHL14</i>	Nonsense	c.763C>T	p.Gln255Ter	47.42	1,242
49	<i>KLHL14</i>	Nonsense	c.735G>A	p.Trp245Ter	42.69	1,225
49	<i>BTG1</i>	Missense	c.123C>G	p.Ser41Arg	42.96	135
49	<i>BTG1</i>	Missense	c.108G>C	p.Gln36His	42.96	135
52	<i>PIMI</i>	Nonsense	c.927C>G	p.Tyr309Ter	33.15	374
52	<i>PRDM1</i>	Nonsense	c.232C>T	p.Gln78Ter	50.64	543
52	<i>ACTB</i>	Missense	c.217C>T	p.His73Tyr	68.18	396
52	<i>CSMD1</i>	Nonsense	c.9254G>A	p.Trp3085Ter	30.49	505
52	<i>ETV6</i>	Missense	c.1256T>G	p.Phe419Cys	33.62	687
52	<i>BCL7A</i>	Missense	c.91T>C	p.Trp31Arg	32.85	137

52	<i>CREBBP</i>	Missense	c.4463C>T	p.Pro1488Leu	48.61	1,473
52	<i>CD79B</i>	Missense	c.590A>G	p.Tyr197Cys	58.42	1,152
52	<i>MYD88</i>	Missense	c.794T>C	p.Leu265Pro	63.94	391
52	<i>BTG2</i>	Missense	c.273G>C	p.Gln91His	42.53	783
56	<i>PIMI</i>	Nonsense	c.382C>T	p.Gln128Ter	55.11	303
56	<i>ACTB</i>	Missense	c.137G>C	p.Gly46Ala	33.64	431
56	<i>CD79B</i>	Missense	c.590A>C	p.Tyr197Ser	34.32	1,110
56	<i>MYD88</i>	Missense	c.794T>C	p.Leu265Pro	43.04	381
56	<i>BTG1</i>	Nonsense	c.168G>A	p.Trp56Ter	57.03	626
56	<i>BTG1</i>	Missense	c.400A>T	p.Thr134Ser	50.12	431
56	<i>BTG1</i>	Missense	c.160C>T	p.His54Tyr	57.03	626
56	<i>BTG1</i>	Missense	c.8C>T	p.Pro3Leu	26.63	612
61	<i>PIMI</i>	Nonsense	c.387C>A	p.Tyr129Ter	48.55	1,584
61	<i>PIMI</i>	Splice	c.513+1G>A		38.99	418
61	<i>KMT2D</i>	Splice	c.10441-2A>G		66.88	2,962
61	<i>IKZF3</i>	Splice	c.826+1G>T		52.79	1,847
61	<i>BTG2</i>	Frameshift	c.100_124delAGGCTTAAGGTCTTCAGCGG GGCGC	p.Arg34SerfsTer59	41.52	2,271
61	<i>MYD88</i>	Missense	c.794T>C	p.Leu265Pro	94.93	592
61	<i>BTG1</i>	Missense	c.14A>T	p.Tyr5Phe	20.82	1,047
82	<i>SOCS1</i>	Frameshift	c.312_330delCGACAGCCGCCAGCGGAAC	p.Asp105AlafsTer7	23.05	564
87	<i>LRP1B</i>	Splice	c.1971-2A>T		47.28	1,303
87	<i>TBLXR1</i>	Missense	c.920A>G	p.His307Arg	50.79	1,262
87	<i>BCL7A</i>	Splice	c.92+1G>A		41.35	237
87	<i>CREBBP</i>	Nonsense	c.5701C>T	p.Gln1901Ter	50.00	92
87	<i>NF1</i>	Nonsense	c.669G>A	p.Trp223Ter	45.19	135
87	<i>BTG2</i>	Missense	c.52G>A	p.Gly18Ser	53.98	2,321
87	<i>BTG2</i>	Missense	c.83G>A	p.Gly28Asp	53.83	2,326
87	<i>BTG2</i>	Missense	c.133G>T	p.Ala45Ser	53.64	2,321
87	<i>BTG2</i>	Missense	c.136C>T	p.Leu46Phe	40.55	2,328
97	<i>PIMI</i>	Nonsense	c.652C>T	p.Gln218Ter	80.38	581
97	<i>PIMI</i>	Nonsense	c.720G>A	p.Trp240Ter	41.68	715
97	<i>PIMI</i>	Nonsense	c.908G>A	p.Trp303Ter	41.99	443
97	<i>PRDM1</i>	Splice	c.291G>C	p.Glu97Asp	51.92	728
97	<i>GRHPR</i>	Splice	c.214+1G>A		41.75	103
97	<i>GRHPR</i>	Splice	c.287+1G>A		36.71	779
97	<i>KMT2D</i>	Frameshift	c.15891_15895dupGGTGC	p.His5299ArgfsTer8	37.80	463

97	<i>CD79B</i>	Missense	c.590A>G	p.Tyr197Cys	33.35	1,475
97	<i>BTG2</i>	Splice	c.142+1G>C		30.43	1,620
97	<i>MYD88</i>	Missense	c.794T>C	p.Leu265Pro	33.06	605
97	<i>MPEG1</i>	Nonsense	c.556C>T	p.Gln186Ter	29.55	714
114	<i>FBXW7</i>	Missense	c.1513C>T	p.Arg505Cys	47.07	2,422
114	<i>IRF4</i>	Missense	c.208C>G	p.Leu70Val	26.67	30
114	<i>PIMI</i>	Frameshift	c.245 249delGTCCC	p.Arg82LeufsTer90	60.07	263
114	<i>PIMI</i>	Frameshift	c.674 702delCGGAAAGGGGAGCCCTGCAA GAGGAGCTG	p.Thr225SerfsTer65	84.02	795
114	<i>CSMD1</i>	Splice	c.9814+1G>A		44.04	965
114	<i>ETV6</i>	Splice	c.12 33+24delTCCTGCTCAGTGTAGCATTA AGGTAAAAATCTTCTCCCCTCCTTCT		50.84	356
114	<i>BCL7A</i>	Missense	c.70G>A	p.Ala24Thr	46.23	106
114	<i>KLHL14</i>	Nonsense	c.562C>T	p.Gln188Ter	33.91	929
114	<i>KLHL14</i>	Nonsense	c.550C>T	p.Gln184Ter	42.80	736
114	<i>MYD88</i>	Missense	c.794T>C	p.Leu265Pro	45.77	627
114	<i>MEF2B</i>	Frameshift	c.396 399dupTGCA	p.Ala134CysfsTer21	46.81	94
114	<i>BTG2</i>	Missense	c.83G>A	p.Gly28Asp	32.40	1,923
114	<i>BTG2</i>	Missense	c.92G>A	p.Ser31Asn	32.40	1,923
126	<i>FAT4</i>	Nonsense	c.3754G>T	p.Gly1252Ter	36.60	806
126	<i>FRY</i>	Frameshift	c.2667delT	p.Leu890TrpfsTer30	20.41	49
132	<i>ITPKB</i>	Nonsense	c.691A>T	p.Lys231Ter	32.56	1,170
132	<i>MYD88</i>	Missense	c.794T>C	p.Leu265Pro	54.79	1,608
132	<i>TBL1XR1</i>	Missense	c.1184A>T	p.Tyr395Phe	44.29	736
132	<i>ACTB</i>	Missense	c.193C>T	p.Leu65Phe	28.15	959
132	<i>GRHPR</i>	Splice	c.214+1G>A		43.33	90
132	<i>ETV6</i>	Splice	c.33+1G>A		54.30	151
132	<i>IRF8</i>	Missense	c.197A>G	p.Lys66Arg	38.90	365
132	<i>BTG2</i>	Missense	c.83G>A	p.Gly28Asp	29.77	2,267
136	<i>MYD88</i>	Missense	c.794T>C	p.Leu265Pro	64.93	211
136	<i>HIST1H1E</i>	Missense	c.308G>A	p.Gly103Asp	22.31	130
136	<i>IGLL5</i>	Frameshift	c.32 41delAGACCCCTGA	p.Glu11GlyfsTer95	33.33	75
136	<i>RBMX</i>	Frameshift	c.1dupA	p.Met1?	36.17	47
136	<i>KMT2D</i>	Nonsense	c.2635G>T	p.Glu879Ter	38.58	127
136	<i>BCL7A</i>	Nonsense	c.92G>A	p.Trp31Ter	28.57	77
137	<i>CD58</i>	Nonsense	c.471C>G	p.Tyr157Ter	35.48	1,581
137	<i>CD58</i>	Nonsense	c.454C>T	p.Arg152Ter	38.45	1,597

137	<i>ITPKB</i>	Nonsense	c.622C>T	p.Gln208Ter	30.72	345
137	<i>MYD88</i>	Missense	c.794T>C	p.Leu265Pro	36.47	987
137	<i>TBL1XR1</i>	Missense	c.1200T>A	p.Ser400Arg	37.32	142
137	<i>TBL1XR1</i>	Missense	c.1124T>A	p.Ile375Lys	40.46	131
137	<i>TBL1XR1</i>	Missense	c.1123A>G	p.Ile375Val	40.46	131
137	<i>PIMI</i>	Nonsense	c.481G>T	p.Glu161Ter	38.11	677
137	<i>CDKN2A</i>	Nonsense	c.330G>A	p.Trp110Ter	36.89	862
137	<i>BCL7A</i>	Missense	c.86G>A	p.Arg29His	31.16	276
137	<i>CIITA</i>	Frameshift	c.3021delC	p.Ser1008GlnfsTer7	39.45	512
137	<i>CD79B</i>	Missense	c.589T>G	p.Tyr197Asp	34.08	1,247
137	<i>GNA13</i>	Nonsense	c.79C>T	p.Gln27Ter	27.96	651
139	<i>MYD88</i>	Missense	c.794T>C	p.Leu265Pro	54.98	1,346
139	<i>PIMI</i>	Nonsense	c.361G>T	p.Glu121Ter	39.10	693
139	<i>PRDM1</i>	Frameshift	c.485_486delTG	p.Val162GlufsTer26	81.73	197
139	<i>ETV6</i>	Splice	c.33+1G>C		83.65	159
139	<i>CREBBP</i>	Missense	c.4472A>C	p.Gln1491Pro	43.25	1,519
139	<i>TP53</i>	Missense	c.761T>A	p.Ile254Asn	82.95	733
139	<i>CD79B</i>	Missense	c.589T>G	p.Tyr197Asp	45.48	1,172
139	<i>IGLL5</i>	Frameshift	c.93_94delGG	p.Ala32HisfsTer59	91.19	590
139	<i>BTG1</i>	Missense	c.116C>T	p.Thr39Ile	46.44	239
144	<i>MYD88</i>	Missense	c.794T>C	p.Leu265Pro	34.62	1,352
144	<i>PRDM1</i>	Splice	c.291G>C	p.Glu97Asp	53.34	718
144	<i>CD79B</i>	Missense	c.590A>G	p.Tyr197Cys	32.83	1,185
144	<i>KLHL14</i>	Nonsense	c.289C>T	p.Gln97Ter	38.02	313
144	<i>BTG1</i>	Missense	c.17C>T	p.Thr6Ile	33.89	773
147	<i>GRHPR</i>	Splice	c.287+1G>A		22.31	1,013
147	<i>ETV6</i>	Splice	c.33+1delG		20.29	138
147	<i>IGLL5</i>	Frameshift	c.212delT	p.Leu71ArgfsTer38	31.77	1,432
147	<i>MYD88</i>	Missense	c.794T>C	p.Leu265Pro	31.90	1,279
147	<i>MPEG1</i>	Nonsense	c.2131C>T	p.Gln711Ter	17.74	248
173	<i>CSMD1</i>	Nonsense	c.585G>A	p.Trp195Ter	42.10	38
174	<i>MYD88</i>	Missense	c.794T>C	p.Leu265Pro	21.72	1,625
174	<i>TBL1XR1</i>	Missense	c.1100G>C	p.Cys367Ser	23.48	1,001
174	<i>PRDM1</i>	Splice	c.291G>A	c.291G>A(p.=)	27.79	662
174	<i>PRDM1</i>	Splice	c.291+1G>A		27.79	662
174	<i>CDKN2A</i>	Nonsense	c.329G>A	p.Trp110Ter	49.78	1,137
174	<i>KMT2D</i>	Nonsense	c.8050C>T	p.Gln2684Ter	25.77	2,716

174	<i>ZFP36L1</i>	Nonsense	c.567C>A	p.Cys189Ter	27.47	1,791
174	<i>KLHL14</i>	Nonsense	c.562C>T	p.Gln188Ter	35.16	2,076
179	<i>NOTCH2</i>	Nonsense	c.7090C>T	p.Gln2364Ter	55.59	1,423
179	<i>BTG2</i>	Frameshift	c.115_116insACTTAAGGTCTTCA	p.Ser39AsnfsTer67	29.44	1,155
179	<i>BTG2</i>	Frameshift	c.115_116insATTTAAGGTCTTCA	p.Ser39AsnfsTer67	20.61	1,155
179	<i>CD79B</i>	Missense	c.590A>C	p.Tyr197Ser	94.96	873
179	<i>GNAI3</i>	Nonsense	c.111C>A	p.Cys37Ter	42.96	568
179	<i>BTG2</i>	Missense	c.83G>A	p.Gly28Asp	40.72	1,159
179	<i>BTG2</i>	Missense	c.121G>C	p.Ala41Pro	40.40	1,161
180	<i>MYD88</i>	Missense	c.794T>C	p.Leu265Pro	42.18	211
180	<i>IRF4</i>	Nonsense	c.178C>T	p.Gln60Ter	34.41	186
180	<i>IRF4</i>	Missense	c.208C>G	p.Leu70Val	94.69	113
180	<i>CD79B</i>	Missense	c.589T>G	p.Tyr197Asp	59.78	184
180	<i>KMT2D</i>	Nonsense	c.12253C>T	p.Gln4085Ter	42.86	252
180	<i>PIMI</i>	Splice	c.355+1G>C		96.80	437
180	<i>ETV6</i>	Splice	c.33+1G>C		54.95	202
180	<i>ETV6</i>	Splice	c.33+1delG		37.62	202
182	<i>GNAI3</i>	Splice	c.283+1G>A		25.63	355
184	<i>MYD88</i>	Missense	c.794T>C	p.Leu265Pro	38.05	1,201
184	<i>TBLIXR1</i>	Missense	c.971C>T	p.Ser324Phe	78.37	1,946
184	<i>PIMI</i>	Splice	c.355+1G>A		39.38	678
184	<i>PIMI</i>	Nonsense	c.432C>A	p.Tyr144Ter	66.80	253
184	<i>PIMI</i>	Frameshift	c.704_711delCCCGCAGC	p.Ala235ValfsTer62	23.55	1,622
184	<i>GRHPR</i>	Splice	c.215-9_217delGCACAACAGGGG		44.26	1,803
184	<i>GRHPR</i>	Frameshift	c.220_221delAA	p.Asn74SerfsTer18	44.36	1,799
184	<i>MPEG1</i>	Nonsense	c.1687C>T	p.Gln563Ter	39.23	989
184	<i>ETV6</i>	Splice	c.31_33+8delAAGGTAAAAAT		80.45	133
184	<i>ZFP36L1</i>	Frameshift	c.750delG	p.Glu250AspfsTer52	29.03	31
184	<i>IGLL5</i>	Frameshift	c.158_179delGAGCCTCAGTTGGAAGCAGC CG	p.Gly53AspfsTer49	62.22	532
184	<i>BTG2</i>	Missense	c.20C>T	p.Thr7Ile	59.84	1,367
184	<i>BTG2</i>	Missense	c.277C>T	p.His93Tyr	37.53	1,327
184	<i>BTG1</i>	Missense	c.197G>A	p.Gly66Asp	43.70	540
184	<i>BTG1</i>	Missense	c.108G>C	p.Gln36His	39.51	205
184	<i>BTG1</i>	Missense	c.91C>T	p.Leu31Phe	40.10	207

189	<i>MYD88</i>	Missense	c.794T>C	p.Leu265Pro	88.47	1,102
189	<i>CD79A</i>	Nonsense	c.553G>T	p.Glu185Ter	52.75	728
189	<i>IGLL5</i>	Splice	c.206+1G>T		35.00	3,177
197	<i>FBXW7</i>	Missense	c.1393C>T	p.Arg465Cys	24.71	603
197	<i>CD79B</i>	Missense	c.589T>A	p.Tyr197Asn	28.35	1,252
197	<i>EP300</i>	Splice	c.1529-2A>T		33.33	222
204	<i>HIST1H1C</i>	Frameshift	c.199_200delGC	p.Ala67CysfsTer5	40.15	259
204	<i>IRF8</i>	Missense	c.67T>C	p.Tyr23His	45.67	1,743
204	<i>CD79B</i>	Missense	c.590A>C	p.Tyr197Ser	38.41	2,114
204	<i>GNAI3</i>	Frameshift	c.93delC	p.Lys32ArgfsTer14	39.48	1,145
204	<i>GNAI3</i>	Frameshift	c.80_89delAGCAACGCAA	p.Gln27ArgfsTer16	39.60	1,149
204	<i>IGLL5</i>	Splice	c.206+17_206+18insTCAGGTAAGGGGCAA GAGATT		49.00	1,945
204	<i>MYD88</i>	Missense	c.794T>C	p.Leu265Pro	46.65	701
204	<i>BTG1</i>	Missense	c.206G>A	p.Cys69Tyr	27.07	1,330

Abbreviations: AA, amino acid; VAF, variant allele frequency

Table S3. Detected pathogenic copy number alterations

Case	Gene	CNA	Log ₂	Case	Gene	CNA	Log ₂	Case	Gene	CNA	Log ₂
1	<i>CDKN2A</i>	Loss	-0.91	49	<i>BCL2</i>	Gain	0.78	139	<i>FLT3</i>	Gain	0.45
1	<i>CDKN2B</i>	Loss	-0.64	49	<i>CD58</i>	Loss	-0.28	139	<i>PRDM1</i>	Loss	-0.75
1	<i>CSMD1</i>	Loss	-0.51	49	<i>CDKN2A</i>	Loss	-3.17	139	<i>SGK1</i>	Loss	-0.89
1	<i>IGLL5</i>	Loss	-0.45	49	<i>CDKN2B</i>	Loss	-4.32	139	<i>TNFAIP3</i>	Loss	-0.94
1	<i>MYC</i>	Gain	0.53	49	<i>CIITA</i>	Loss	-0.74	139	<i>TP53</i>	Loss	-0.82
1	<i>PRDM1</i>	Loss	-0.37	49	<i>ETV6</i>	Loss	-0.95	144	<i>CDKN2A</i>	Loss	-1.12
1	<i>SGK1</i>	Loss	-0.47	49	<i>IGLL5</i>	Loss	-3.46	144	<i>CDKN2B</i>	Loss	-1.68
1	<i>TNFAIP3</i>	Loss	-0.52	49	<i>MALT1</i>	Gain	0.78	144	<i>PRDM1</i>	Loss	-0.53
10	<i>BCL7A</i>	Loss	-0.45	52	<i>CDKN2A</i>	Loss	-1.28	144	<i>SGK1</i>	Loss	-0.36
10	<i>CDKN2A</i>	Loss	-0.68	52	<i>CDKN2B</i>	Loss	-2.51	144	<i>STAT6</i>	Gain	0.80
10	<i>CDKN2B</i>	Loss	-1.29	52	<i>MEF2B</i>	Loss	-0.61	144	<i>TNFAIP3</i>	Loss	-0.55
10	<i>ETV6</i>	Loss	-0.54	56	<i>CDKN2A</i>	Loss	-2.61	179	<i>STAT6</i>	Gain	0.83
10	<i>KMT2D</i>	Loss	-0.65	56	<i>CDKN2B</i>	Loss	-3.49	179	<i>CDKN2A</i>	Loss	-3.74
10	<i>PRDM1</i>	Loss	-1.30	56	<i>PRDM1</i>	Loss	-2.36	179	<i>CDKN2B</i>	Loss	-3.79
12	<i>CDKN2A</i>	Loss	-0.78	61	<i>BCL7A</i>	Loss	-0.56	180	<i>BCL2</i>	Gain	0.87
12	<i>CDKN2B</i>	Loss	-0.84	61	<i>CDKN2A</i>	Loss	-3.11	180	<i>BCL7A</i>	Loss	-0.69
12	<i>IGLL5</i>	Loss	-0.49	61	<i>CDKN2B</i>	Loss	-2.27	180	<i>CD274</i>	Gain	0.74
12	<i>PIMI1</i>	Loss	-0.55	61	<i>IGLL5</i>	Loss	-1.43	180	<i>CDKN2A</i>	Loss	-3.09
12	<i>PRDM1</i>	Loss	-0.36	61	<i>PRDM1</i>	Loss	-0.92	180	<i>CDKN2B</i>	Loss	-1.34
12	<i>SGK1</i>	Loss	-0.33	61	<i>SGK1</i>	Loss	-0.70	180	<i>MALT1</i>	Gain	0.55
12	<i>TNFAIP3</i>	Loss	-0.37	61	<i>TNFAIP3</i>	Loss	-0.90	180	<i>SETBP1</i>	Gain	0.69
22	<i>CDKN2A</i>	Loss	-2.48	87	<i>CDKN2A</i>	Loss	-4.01	184	<i>ARID2</i>	Loss	-0.75
22	<i>CDKN2B</i>	Loss	-2.33	87	<i>CDKN2B</i>	Loss	-4.51	184	<i>CDKN2A</i>	Loss	-2.52
22	<i>CSMD1</i>	Loss	-0.76	97	<i>CDKN2A</i>	Loss	-3.14	184	<i>CDKN2B</i>	Loss	-2.35
22	<i>ETV6</i>	Loss	-0.68	97	<i>CDKN2B</i>	Loss	-1.54	184	<i>CSMD1</i>	Loss	-0.61
22	<i>IGLL5</i>	Loss	-2.77	97	<i>ETV6</i>	Loss	-1.54	184	<i>ETV6</i>	Loss	-0.51
22	<i>MEF2B</i>	Loss	-0.52	97	<i>NFKBIZ</i>	Gain	0.47	184	<i>PRDM1</i>	Loss	-0.82
22	<i>PRDM1</i>	Loss	-0.81	114	<i>CDKN2A</i>	Loss	-1.05	184	<i>SGK1</i>	Loss	-1.10
26	<i>CDKN2A</i>	Loss	-0.32	114	<i>CDKN2B</i>	Loss	-1.66	184	<i>TNFAIP3</i>	Loss	-0.81
26	<i>ETV6</i>	Loss	-0.42	114	<i>MPEG1</i>	Loss	-0.78	189	<i>MCL1</i>	Gain	0.81
26	<i>IGLL5</i>	Loss	-1.69	132	<i>CDKN2A</i>	Loss	-1.90	189	<i>BRAF</i>	Gain	0.38
26	<i>MALT1</i>	Gain	0.60	132	<i>CDKN2B</i>	Loss	-1.75	189	<i>STAT6</i>	Gain	0.38

26	<i>SETBP1</i>	Gain	0.56	132	<i>NFKBIZ</i>	Gain	0.50	189	<i>PRDM1</i>	Loss	-0.75
31	<i>BCL2</i>	Gain	0.48	132	<i>RHOA</i>	Gain	0.81	189	<i>SGK1</i>	Loss	-0.71
31	<i>CDKN2A</i>	Loss	-1.46	132	<i>SGK1</i>	Loss	-0.71	189	<i>TNFAIP3</i>	Loss	-0.72
31	<i>CDKN2B</i>	Loss	-1.67	132	<i>TNFAIP3</i>	Loss	-0.91	197	<i>STAT6</i>	Gain	0.63
31	<i>MALT1</i>	Gain	0.51	136	<i>CDKN2A</i>	Loss	-0.83	197	<i>CDKN2A</i>	Loss	-1.04
31	<i>PRDM1</i>	Loss	-0.56	136	<i>CDKN2B</i>	Loss	-0.85	197	<i>IGLL5</i>	Loss	-1.11
31	<i>SETBP1</i>	Gain	0.53	136	<i>PRDM1</i>	Loss	-0.50	204	<i>CDKN2A</i>	Loss	-4.93
31	<i>TMSB4X</i>	Gain	0.96	136	<i>SGK1</i>	Loss	-0.79	204	<i>CDKN2B</i>	Loss	-2.11
39	<i>CD274</i>	Gain	0.68	136	<i>TNFAIP3</i>	Loss	-0.38	204	<i>CREBBP</i>	Loss	-0.80
39	<i>CDKN2A</i>	Loss	-3.86	137	<i>SGK1</i>	Loss	-0.79	204	<i>IGLL5</i>	Loss	-1.19
39	<i>CDKN2B</i>	Loss	-4.63	139	<i>CDKN2A</i>	Loss	-2.85	204	<i>PRDM1</i>	Loss	-0.90
39	<i>ETV6</i>	Loss	-2.81	139	<i>CDKN2B</i>	Loss	-3.62	204	<i>SGK1</i>	Loss	-0.93
39	<i>IGLL5</i>	Loss	-0.86	139	<i>ETV6</i>	Loss	-0.57	204	<i>TNFAIP3</i>	Loss	-1.11

Abbreviations: CNA, copy number alteration

Table S4. Relationship between *ETV6* loss and clinical findings

Factors	<i>ETV6</i> loss		p-value
	Positive (n = 8)	Negative (n = 27)	
Sex, male/female	3/5	11/16	1
Age, median (range), years	71.5 (45–83)	69 (43–84)	0.70
Laterality, unilateral/bilateral	3/5	12/15	1
IL-10 level (pg/mL), median (range)	890 (17–5005)	1008 (10–130,125)	0.50
IL-10/IL-6 ratio	12.6 (0.29–98.1)	15.6 (0.46–1161.8)	0.26
Cytopathology positive (class \geq IIIb)	6/2	17/10	0.69
Detection of B-cell clonality (FCM analysis)	5/1	18/6	1
Positive for <i>IGH</i> rearrangement (PCR)	8/0	20/6	0.30
WBC (/ μ L), median (range)	5950 (4500–13,000)	6200 (3600–12,400)	0.84
ANC (/ μ L), median (range)	3735 (2547–10,946)	4018 (2051–11,284)	0.95
ALC (/ μ L), median (range)	1905 (1363–2539)	1488 (792–3834)	0.24
LDH (U/L), median (range)	220.5 (163–376)	199 (141–274)	0.38
sIL-2R (U/mL), median (range)	269.5 (208.4–4040)	321 (107–762)	0.40
CRP (mg/dL), median (range)	0.06 (0.02–0.48)	0.05 (0.02–0.54)	0.41

p-values < 0.05 were considered statistically significant.

Abbreviations: ALC, absolute lymphocyte count; ANC, absolute neutrophil count; CRP, C-reactive protein; FCM, flow cytometry; IL, interleukin; LDH, lactate dehydrogenase; PCR, polymerase chain reaction; sIL-2R, soluble interleukin-2 receptor, WBC, white blood cell

Table S5. Relationship between *PRDMI* alteration and clinical findings

Factors	<i>PRDMI</i> alteration		p-value
	Positive (n = 17)	Negative (n = 18)	
Sex, male/female	9/8	5/13	0.18
Age, median (range), years	72 (45–83)	69.5 (43–84)	0.47
Laterality, unilateral/bilateral	5/12	10/8	0.18
IL-10 level (pg/mL), median (range)	738 (137–130,125)	1192 (10–10,596)	0.64
IL-10/IL-6 ratio	17.4 (1.2–1161.8)	13.0 (0.29–190.6)	0.22
Cytopathology positive (class \geq IIIb)	12/5	11/7	0.73
B-cell clonality (FCM analysis)	11/4	12/3	1
Positive for <i>IGH</i> gene rearrangement (PCR)	12/4	16/2	0.39
WBC (/ μ L), median (range)	6000 (4100–13000)	6200 (3600–12,400)	0.87
ANC (/ μ L), median (range)	3870 (2378–10946)	3959 (2051–11,284)	0.88
ALC (/ μ L), median (range)	1488 (968–2539)	1632.5 (792–3834)	0.82
LDH (U/L), median (range)	199 (157–376)	212.5 (141–274)	0.88
sIL-2R (U/mL), median (range)	287.1 (125–4040)	341.5 (107–762)	0.31
CRP (mg/dL), median (range)	0.04 (0.02–0.48)	0.065 (0.02–0.54)	0.69

p-values < 0.05 were considered statistically significant.

Abbreviations: ALC, absolute lymphocyte count; ANC, absolute neutrophil count; CRP, C-reactive protein; FCM, flow cytometry; IL, interleukin; LDH, lactate dehydrogenase; PCR, polymerase chain reaction; sIL-2R, soluble interleukin-2 receptor; WBC, white blood cell

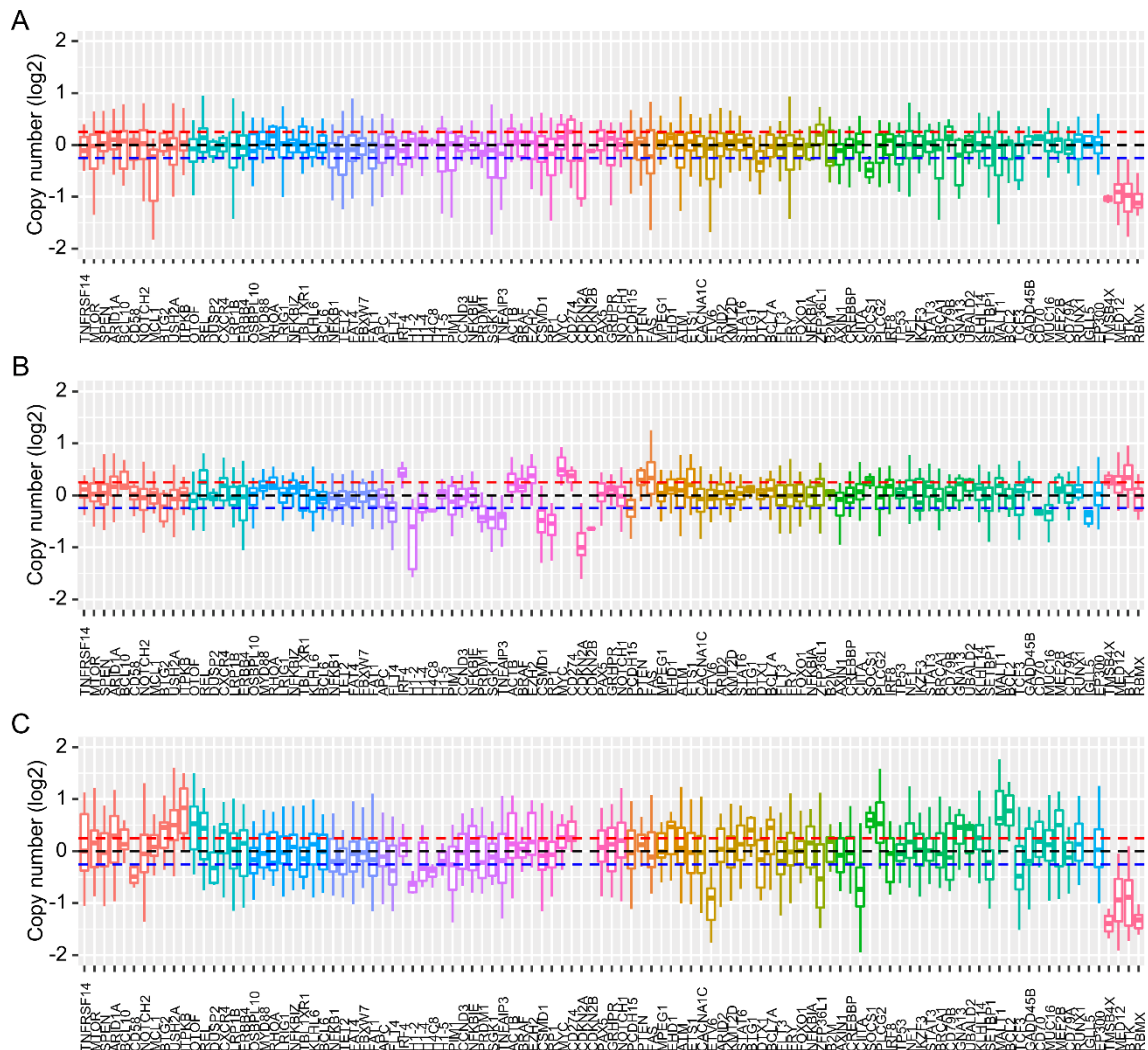
Table S6. Pathogenic gene alteration in primary vitreoretinal lymphoma patients with central nervous system progression

Case	Vitreous humor					Brain				
	Gene	Mutation type	cDNA change	AA change	VAF	Gene	Mutation type	cDNA change	AA change	VAF
39	<i>MYD88</i>	Missense	c.794T>C	p.Leu265Pro	39.48	<i>MYD88</i>	Missense	c.794T>C	p.Leu265Pro	90.42
	<i>KMT2D</i>	Nonsense	c.12844C>T	p.Arg4282Ter	34.29	<i>KMT2D</i>	Nonsense	c.12844C>T	p.Arg4282Ter	70.33
	<i>CD274</i>			Gain		<i>CD274</i>			Gain	
	<i>CDKN2A</i>			Loss		<i>CDKN2A</i>			Loss	
	<i>CDKN2B</i>			Loss		<i>CDKN2B</i>			Loss	
	<i>IGLL5</i>			Loss		<i>IGLL5</i>			Loss	
	<i>ETV6</i>			Loss				-		
				-		<i>ACTB</i>			Gain	
				-		<i>CD58</i>	Frameshift	c.218delC	p.Ala73ValfsTer11	91.62
				-		<i>IRF4</i>	Missense	c.170C>T	p.Ala57Val	64.48
				-		<i>HIST1H1C</i>	Missense	c.347C>G	p.Ala116Gly	94.51
				-		<i>HIST1H4H</i>	Missense	c.28G>T	p.Gly10Cys	34.31
				-		<i>MYC</i>	Missense	c.63C>G	p.Ser21Arg	63.02
				-		<i>MYC</i>	Missense	c.106C>T	p.Pro36Ser	63.35
				-		<i>MYC</i>	Missense	c.650G>C	p.Ser217Thr	62.87
				-		<i>CD79B</i>	Missense	c.589T>C	p.Tyr197His	57.61
			-		<i>BRAF</i>			Gain		
			-		<i>STAT6</i>			Gain		
			-		<i>B2M</i>			Loss		
56	<i>ACTB</i>	Missense	c.137G>C	p.Gly46Ala	33.64	<i>ACTB</i>	Missense	c.137G>C	p.Gly46Ala	40.37
	<i>CD79B</i>	Missense	c.590A>C	p.Tyr197Ser	34.32	<i>CD79B</i>	Missense	c.590A>C	p.Tyr197Ser	39.56
	<i>MYD88</i>	Missense	c.794T>C	p.Leu265Pro	43.04	<i>MYD88</i>	Missense	c.794T>C	p.Leu265Pro	40.16
	<i>BTG1</i>	Missense	c.400A>T	p.Thr134Ser	50.12	<i>BTG1</i>	Missense	c.400A>T	p.Thr134Ser	39.05
	<i>BTG1</i>	Missense	c.160C>T	p.His54Tyr	57.03	<i>BTG1</i>	Missense	c.160C>T	p.His54Tyr	38.59
	<i>BTG1</i>	Nonsense	c.168G>A	p.Trp56Ter	57.03	<i>BTG1</i>	Nonsense	c.168G>A	p.Trp56Ter	38.59
	<i>BTG1</i>	Missense	c.8C>T	p.Pro3Leu	26.63	<i>BTG1</i>	Missense	c.8C>T	p.Pro3Leu	35.94
	<i>PRDMI</i>			Loss		<i>PRDMI</i>			Loss	
	<i>CDKN2A</i>			Loss		<i>CDKN2A</i>			Loss	
	<i>CDKN2B</i>			Loss		<i>CDKN2B</i>			Loss	
	<i>PIMI</i>	Nonsense	c.382C>T	p.Gln128Ter	55.11			-		

	<i>KMT2D</i>			Loss					-	
	<i>BCL7A</i>			Loss					-	
				-		<i>BTG1</i>	Missense	c.316G>A	p.Val106Ile	42.37
				-		<i>GNAI3</i>	Nonsense	c.79C>T	p.Gln27Ter	41.29
82	<i>SOCS1</i>	Frameshift	c.312_330delCG ACAGCCGCCA GCGGAAC	p.Asp105AlafsTer7	23.05	<i>SOCS1</i>	Frameshift	c.312_330delCGACAGC CGCCAGCGGAAC	p.Asp105AlafsTer7	49.62
				-		<i>MYD88</i>			Gain	
				-		<i>RHOA</i>			Gain	
				-		<i>TET2</i>			Loss	
				-		<i>FAT4</i>			Loss	
				-		<i>FBXW7</i>			Loss	
				-		<i>FAT1</i>			Loss	
				-		<i>CDKN2A</i>			Loss	
				-		<i>CDKN2B</i>			Loss	
				-		<i>IGLL5</i>			Loss	
				-		<i>MYD88</i>	Missense	c.794T>C	p.Leu265Pro	42.32
				-		<i>HIST1H1E</i>	Missense	c.536C>T	p.Ala179Val	24.25
				-		<i>PIM1</i>	Splice	c.356-1G>A		40.08
				-		<i>PRDM1</i>	Nonsense	c.1230C>A	p.Tyr410Ter	78.49
				-		<i>ACTB</i>	Missense	c.585G>C	p.Glu195Asp	31.11
				-		<i>CSMD1</i>	Splice	c.86-2A>G		26.09
				-		<i>BTG1</i>	Missense	c.136G>A	p.Glu46Lys	38.39
				-		<i>IGLL5</i>	Splice	c.206+1G>C		37.45
97	<i>PIM1</i>	Nonsense	c.720G>A	p.Trp240Ter	41.68	<i>PIM1</i>	Nonsense	c.720G>A	p.Trp240Ter	44.93
	<i>PIM1</i>	Nonsense	c.908G>A	p.Trp303Ter	41.99	<i>PIM1</i>	Nonsense	c.908G>A	p.Trp303Ter	43.76
	<i>GRHPR</i>	Splice	c.287+1G>A		36.71	<i>GRHPR</i>	Splice	c.287+1G>A		47.28
	<i>KMT2D</i>	Frameshift	c.15891_15895dup pGGTGC	p.His5299ArgfsTer8	37.80	<i>KMT2D</i>	Frameshift	c.15891_15895dupGGTG C	p.His5299ArgfsTer8	52.79
	<i>CD79B</i>	Missense	c.590A>G	p.Tyr197Cys	33.35	<i>CD79B</i>	Missense	c.590A>G	p.Tyr197Cys	37.82
	<i>BTG2</i>	Splice	c.142+1G>C		30.43	<i>BTG2</i>	Splice	c.142+1G>C		39.49
	<i>MYD88</i>	Missense	c.794T>C	p.Leu265Pro	33.06	<i>MYD88</i>	Missense	c.794T>C	p.Leu265Pro	47.34
	<i>MPEG1</i>	Nonsense	c.556C>T	p.Gln186Ter	29.55	<i>MPEG1</i>	Nonsense	c.556C>T	p.Gln186Ter	42.65
	<i>PRDM1</i>	Splice	c.291G>C	p.Glu97Asp	51.92	<i>PRDM1</i>	Missense	c.291G>C	p.Glu97Asp	78.68
	<i>CDKN2A</i>			Loss		<i>CDKN2A</i>			Loss	

<i>CDKN2B</i>	Loss				<i>CDKN2B</i>	Loss		
<i>PIM1</i>	Nonsense	c.652C>T	p.Gln218Ter	80.38	-			
<i>GRHRP</i>	Splice	c.214+1G>A		41.75	-			
<i>ETV6</i>	Loss				-			
<i>NFKBIZ</i>	Gain				-			
-					<i>PIM1</i>	Splice	c.356-9 357delCTTTCCTAGGC	29.60
-					<i>MYC</i>	Missense	c.486G>T	p.Glu162Asp 48.26
-					<i>STAT6</i>	Gain		
-					<i>IGLL5</i>	Loss		

Abbreviations: AA, amino acid; CNS, central nervous system; VAF, variant allele frequency



Supplemental Figure 1. Representative copy number plot. Copy numbers of each amplicon were shown as boxplot organized by the gene level. Results of uveitis sample (control) and two PVRL cases (Case 1 and 49) are shown in (A) and (B) and (C), respectively. Black dotted line indicates copy number neutral value. Red and blue dotted lines are thresholds for gain and loss, respectively.

Supplementary references

1. Levy N, Nelson J, Meyer P, Lukes RJ, Parker JW. Reactive lymphoid hyperplasia with single class (monoclonal) surface immunoglobulin. *Am J Clin Pathol.* 1983;80(3):300-308.
2. Bolger AM, Lohse M, Usadel B. Trimmomatic: a flexible trimmer for Illumina sequence data. *Bioinformatics.* 2014;30(15):2114-2120.
3. Li H, Durbin R. Fast and accurate short read alignment with Burrows-Wheeler transform. *Bioinformatics.* 2009;25(14):1754-1760.
4. Okonechnikov K, Conesa A, Garcia-Alcalde F. Qualimap 2: advanced multi-sample quality control for high-throughput sequencing data. *Bioinformatics.* 2016;32(2):292-294.
5. McKenna A, Hanna M, Banks E, et al. The Genome Analysis Toolkit: a MapReduce framework for analyzing next-generation DNA sequencing data. *Genome Res.* 2010;20(9):1297-1303.
6. Najima Y, Sadato D, Harada Y, et al. Prognostic impact of TP53 mutation, monosomal karyotype, and prior myeloid disorder in nonremission acute myeloid leukemia at allo-HSCT. *Bone Marrow Transplant.* 2021;56(2):334-346.
7. Talevich E, Shain AH, Botton T, Bastian BC. CNVkit: Genome-Wide Copy Number Detection and Visualization from Targeted DNA Sequencing. *PLoS Comput Biol.* 2016;12(4):e1004873.
8. Lohr JG, Stojanov P, Lawrence MS, et al. Discovery and prioritization of somatic mutations in diffuse large B-cell lymphoma (DLBCL) by whole-exome sequencing. *Proc Natl Acad Sci U S A.* 2012;109(10):3879-3884.
9. Wang X, Su W, Gao Y, et al. A pilot study of the use of dynamic analysis of cell-free DNA from aqueous humor and vitreous fluid for the diagnosis and treatment monitoring of vitreoretinal lymphomas. *Haematologica.* 2022;107(9):2154-2162.
10. Zhang F, Lu YJ, Malley R. Multiple antigen-presenting system (MAPS) to induce comprehensive B- and T-cell immunity. *Proc Natl Acad Sci U S A.* 2013;110(33):13564-13569.
11. Schmitz R, Wright GW, Huang DW, et al. Genetics and Pathogenesis of Diffuse Large B-Cell Lymphoma. *N Engl J Med.* 2018;378(15):1396-1407.
12. Challa-Malladi M, Lieu YK, Califano O, et al. Combined genetic inactivation of beta2-Microglobulin and CD58 reveals frequent escape from immune recognition in diffuse large B cell lymphoma. *Cancer Cell.* 2011;20(6):728-740.
13. Morin RD, Mendez-Lago M, Mungall AJ, et al. Frequent mutation of histone-modifying genes in non-Hodgkin lymphoma. *Nature.* 2011;476(7360):298-303.
14. Balinas-Gavira C, Rodriguez MI, Andrades A, et al. Frequent mutations in the amino-terminal domain of BCL7A impair its tumor suppressor role in DLBCL. *Leukemia.* 2020;34(10):2722-2735.
15. Lee J, Kim B, Lee H, et al. Whole exome sequencing identifies mutational signatures of vitreoretinal lymphoma. *Haematologica.* 2020;105(9):e458-460.
16. Bonzheim I, Sander P, Salmeron-Villalobos J, et al. The molecular hallmarks of primary and

secondary vitreoretinal lymphoma. *Blood Adv.* 2022;6(5):1598-1607.

17. Mlynarczyk C, Teater M, Pae J, et al. BTG1 mutation yields supercompetitive B cells primed for malignant transformation. *Science.* 2023;379(6629):eabj7412.
18. Hu N, Wang F, Sun T, et al. Follicular Lymphoma-associated BTK Mutations are Inactivating Resulting in Augmented AKT Activation. *Clin Cancer Res.* 2021;27(8):2301-2313.
19. Schmitz R, Young RM, Ceribelli M, et al. Burkitt lymphoma pathogenesis and therapeutic targets from structural and functional genomics. *Nature.* 2012;490(7418):116-120.
20. Kataoka K, Shiraishi Y, Takeda Y, et al. Aberrant PD-L1 expression through 3'-UTR disruption in multiple cancers. *Nature.* 2016;534(7607):402-406.
21. Davis RE, Ngo VN, Lenz G, et al. Chronic active B-cell-receptor signalling in diffuse large B-cell lymphoma. *Nature.* 2010;463(7277):88-92.
22. Nayyar N, White MD, Gill CM, et al. MYD88 L265P mutation and CDKN2A loss are early mutational events in primary central nervous system diffuse large B-cell lymphomas. *Blood Adv.* 2019;3(3):375-383.
23. Mottok A, Woolcock B, Chan FC, et al. Genomic Alterations in CIITA Are Frequent in Primary Mediastinal Large B Cell Lymphoma and Are Associated with Diminished MHC Class II Expression. *Cell Rep.* 2015;13(7):1418-1431.
24. Escudero-Esparza A, Bartoschek M, Gialeli C, et al. Complement inhibitor CSMD1 acts as tumor suppressor in human breast cancer. *Oncotarget.* 2016;7(47):76920-76933.
25. Treon SP, Tripsas CK, Meid K, et al. Ibrutinib in previously treated Waldenstrom's macroglobulinemia. *N Engl J Med.* 2015;372(15):1430-1440.
26. de Miranda NF, Georgiou K, Chen L, et al. Exome sequencing reveals novel mutation targets in diffuse large B-cell lymphomas derived from Chinese patients. *Blood.* 2014;124(16):2544-2553.
27. Bonetti P, Testoni M, Scandurra M, et al. Deregulation of ETS1 and FLI1 contributes to the pathogenesis of diffuse large B-cell lymphoma. *Blood.* 2013;122(13):2233-2241.
28. Gronbaek K, Straten PT, Ralfkiaer E, et al. Somatic Fas mutations in non-Hodgkin's lymphoma: association with extranodal disease and autoimmunity. *Blood.* 1998;92(9):3018-3024.
29. Laginestra MA, Cascione L, Motta G, et al. Whole exome sequencing reveals mutations in FAT1 tumor suppressor gene clinically impacting on peripheral T-cell lymphoma not otherwise specified. *Mod Pathol.* 2020;33(2):179-187.
30. Cai J, Feng D, Hu L, et al. FAT4 functions as a tumour suppressor in gastric cancer by modulating Wnt/beta-catenin signalling. *Br J Cancer.* 2015;113(12):1720-1729.
31. Liu N, Gao M. FLT4 Mutations Are Associated with Segmental Lymphatic Dysfunction and Initial Lymphatic Aplasia in Patients with Milroy Disease. *Genes (Basel).* 2021;12(10):
32. Trinh DL, Scott DW, Morin RD, et al. Analysis of FOXO1 mutations in diffuse large B-cell lymphoma. *Blood.* 2013;121(18):3666-3674.

33. Mai Z, Yuan J, Yang H, et al. Inactivation of Hippo pathway characterizes a poor-prognosis subtype of esophageal cancer. *JCI Insight*. 2022;7(16):
34. Muppidi JR, Schmitz R, Green JA, et al. Loss of signalling via Galpha13 in germinal centre B-cell-derived lymphoma. *Nature*. 2014;516(7530):254-258.
35. Andrades A, Alvarez-Perez JC, Patino-Mercau JR, Cuadros M, Balinas-Gavira C, Medina PP. Recurrent splice site mutations affect key diffuse large B-cell lymphoma genes. *Blood*. 2022;139(15):2406-2410.
36. Li H, Kaminski MS, Li Y, et al. Mutations in linker histone genes HIST1H1 B, C, D, and E; OCT2 (POU2F2); IRF8; and ARID1A underlying the pathogenesis of follicular lymphoma. *Blood*. 2014;123(10):1487-1498.
37. Cherian MA, Olson S, Sundaramoorthi H, et al. An activating mutation of interferon regulatory factor 4 (IRF4) in adult T-cell leukemia. *J Biol Chem*. 2018;293(18):6844-6858.
38. Reddy A, Zhang J, Davis NS, et al. Genetic and Functional Drivers of Diffuse Large B Cell Lymphoma. *Cell*. 2017;171(2):481-494 e415.
39. Choi J, Phelan JD, Wright GW, et al. Regulation of B cell receptor-dependent NF-kappaB signaling by the tumor suppressor KLHL14. *Proc Natl Acad Sci U S A*. 2020;117(11):6092-6102.
40. Pon JR, Wong J, Saberi S, et al. MEF2B mutations in non-Hodgkin lymphoma dysregulate cell migration by decreasing MEF2B target gene activation. *Nat Commun*. 2015;6(7953).
41. Weniger MA, Kuppers R. Molecular biology of Hodgkin lymphoma. *Leukemia*. 2021;35(4):968-981.
42. Dobashi A, Togashi Y, Tanaka N, et al. TP53 and OSBPL10 alterations in diffuse large B-cell lymphoma: prognostic markers identified via exome analysis of cases with extreme prognosis. *Oncotarget*. 2018;9(28):19555-19568.
43. Gu Z, Churchman ML, Roberts KG, et al. PAX5-driven subtypes of B-progenitor acute lymphoblastic leukemia. *Nat Genet*. 2019;51(2):296-307.
44. Zheng T, Zhou H, Li X, et al. RBMX is required for activation of ATR on repetitive DNAs to maintain genome stability. *Cell Death Differ*. 2020;27(11):3162-3176.
45. Koskela HL, Eldfors S, Ellonen P, et al. Somatic STAT3 mutations in large granular lymphocytic leukemia. *N Engl J Med*. 2012;366(20):1905-1913.
46. Yildiz M, Li H, Bernard D, et al. Activating STAT6 mutations in follicular lymphoma. *Blood*. 2015;125(4):668-679.
47. Venturutti L, Teater M, Zhai A, et al. TBL1XR1 Mutations Drive Extranodal Lymphoma by Inducing a Pro-tumorigenic Memory Fate. *Cell*. 2020;182(2):297-316 e227.
48. Kato M, Sanada M, Kato I, et al. Frequent inactivation of A20 in B-cell lymphomas. *Nature*. 2009;459(7247):712-716.
49. Wu F, Watanabe N, Tzioni MM, et al. Thyroid MALT lymphoma: self-harm to gain potential T-

cell help. *Leukemia*. 2021;35(12):3497-3508.